GEOPHYSICAL RESEARCH LETTERS, VOL. 26, NO. 6, PAGES 667-670, MARCH 15, 1999

Observation of topside ionospheric MF/HF radio emission from space

S. D. Bale

Space Sciences Laboratory, University of California, Berkeley

Abstract. We present observations of MF/HF ionospheric radio emission observed between 4-7 R_e in the terrestrial magnetosphere by the Wind spacecraft. During a perigee pass, and AKR episode, two distinct radio signatures are observed: an intense, sporadic emission near $f \approx 1.8$ MHz, and a more steady and weaker emission near $f \approx 4.4$ MHz. These emissions show characteristics similar to ground observations of ionospheric 'auroral roar', although to propagate to the spacecraft they must have been generated above the ionospheric F-layer peak. We suggest that the emissions are generated on the topside ionosphere where the condition $f_{uh} \approx nf_{ce}$ is met. These observations represent a new component of the natural terrestrial radio spectrum as viewed from space.

Introduction

Observations of ionospheric radio emission in the MF (0.3-3 MHz) and HF (3-30 MHz) bands from space are very rare. *James et al.* [1974] reported emission at 2 MHz and 4 MHz by the ISIS spacecraft (apogee ≤ 0.5 R_e), this is the only previous observation known to us. *LaBelle et al.* [1989] used radio receivers on the AMPTE/IRM spacecraft to search systematically for ionospheric radio emission between 1-5.6 MHz; other than confirming previous observations of harmonic AKR [e. g. *Benson*, 1982], they found no convincing evidence of natural ionospheric emission at the orbit of IRM. Observations of radio emission propagating to the ground from the bottomside ionosphere were made by *Kellogg and Monson* [1979] and interpreted as emission at twice the local electron cyclotron frequency ($2f_{ce}$) from the active aurora overhead. *Weatherwax et al.* [1993] reported emission at both $2f_{ce}$ and $3f_{ce}$ and polarization measurements [*Shepard et al.*, 1997] show that this emission is polarized in the *o*-mode, which argues against direct emission from an electron cyclotron maser instability (ECMI) [e. g. *Willes et al.*, 1998].

In this letter, we present observations of ionospheric radio emission detected while the Wind spacecraft was at distances of 4-7 R_e from Earth. The emissions appear similar in morphology to bottomside auroral roar observations; however it is unlikely that bottomside sources would be visible to the spacecraft and we propose that the emissions are generated on the topside of the ionospheric F-layer. An intense band of MF emission, near 1.8 MHz, is likely to be generated at about 1000 km altitude where $f_{uh} \approx 2f_{ce}$. HF emission near 4.5 MHz is then probably generated at near 400 km where $f_{uh} \approx 3f_{ce}$. Concomitant AKR observations occur at frequencies that preclude the interpretation of these emissions as harmonic AKR, although there is some evidence of harmonic structure in the AKR spectrum. We believe that this is the first unequivocal observation of terrestrial MF/HF ionospheric radio emission beyond 1 R_e.

Observations and Analysis

In Figure 1 we show spectrograms of data from the WAVES experiment on the Wind spacecraft [*Bougeret et al.*, 1995] measured on November 13, 1998. Panel (a) shows radio wave measurements in the range 1-5.5 MHz by the RAD2 receiver; this is data from the spin-plane antenna (15 m tip-to-tip) and shows spin modulation due to the directionality of the signals, an effect that rules out local generation. Panel (b) is the RAD1 receiver, covering the range 20-1040 kHz. The bottom panel (c) shows the RAD2_Z (z-axis) signal after background subtraction. The background is taken to be the average signal during the interval 14:05-14:30 UT; standard deviations are also calculated. RAD2 spectra are 20 second averages, so the background comprises 75 spectra. Although the RAD2_Z has lower gain, due to a shorter antenna, the lack of spin modulation allows a better display after background subtraction.

Beginning at approximately 14:50 UT is a radio source peaked at about 1.8 MHz; the emission is fairly intense, sporadic, and the peak frequency changes slightly with time. This is labeled as 'MF Emission' in panel (c) of Figure 1. The relatively sporadic and broadband nature of the signal distinguishes it from man-made sources like those visible near 1.5 MHz, beginning at 16:10 UT. Observed shortwave radio transmitters tend to be very narrowband ($\delta f/f \approx 0.001$), constant frequency, and begin and end transmission abruptly (often on UT hour boundaries). A second component, beginning at about 15:30 UT, appears at near 4.4 MHz and is labeled 'HF Emission' in Figure 1. This signal is also relatively broadband, but weaker. If generated near local plasma resonances, these emissions must come from the topside ionosphere. There are no plasmas with f_{ce} and f_{pe} at a few MegaHertz between the ionosphere and the solar corona; no interplanetary type II activity was observed on this day. The RAD1 and TNR spectograms (panels (b) and (c)) show concomitant AKR observations. During the interval of the observations in Figure 1, the spacecraft moves from 7 R_e (0.78, 6.98, -0.33 GSE) to about 4.2 R_e (-2.41, 3.45, -0.47 GSE). Spacecraft radial distance and local time (in fractional hours) are included on the abscissa in Figure 1.

Figure 2 shows measured power spectra during the two events from the RAD1 (0.02-1.04 MHz) and RAD2 (> 1.075 MHz) receivers. The top panel is a spectrum taken at 15:08

Paper number 1999GL900048.
0094-8276/99/1999GL900048$05.00

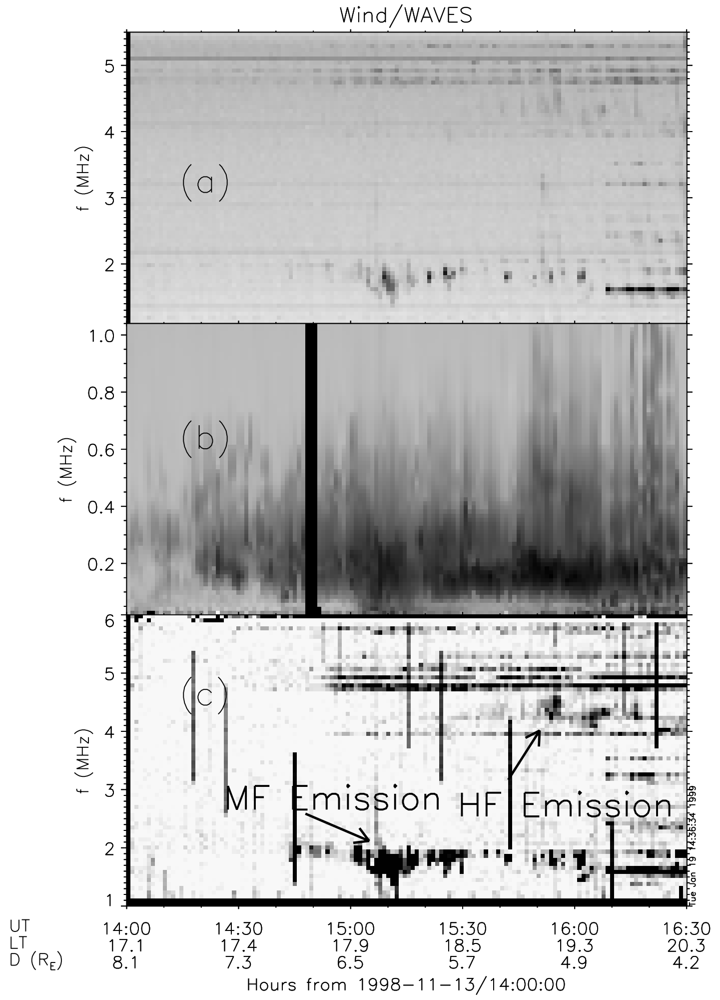

Figure 1. Spectrogram of Wind/WAVES data on 1998-11-13. Panel (a) is data from the RAD2 instrument showing MF radio emission beginning at 14:50 UT at 1.8 MHz. Panel (b) from the RAD1 receiver, shows AKR observations peaked at around 175 kHz. The bottom panel (c) is RAD2 data from z-axis dipole with the background subtracted. Local time and radial distance of the spacecraft are also given on the abscissa. Here the MF and HF (4.4 MHz) emissions are visible; the peak frequency of these signals wanders with time. The spectra are similar to ground-based observations of bottomside ionospheric 'auroral roar' emissions.

UT, during the MF emission event. AKR emission can be seen peaked at $f_{AKR} \approx 175$ kHz; the MF emission is seen peaked at $f_{MF} \approx 1.8$ MHz. The error bars on the RAD2 data in Figure 2 are ± 3 σ variations from the background data. The FWHM bandwidth of the MF peak is $\delta f/f \approx 0.14$ and the peak power is roughly 2 10^{-17} W/m^2Hz. The bottom panel of Figure 2 shows the HF emission event at 15:54 UT with a broad peak above background near $f_{HF} \approx 4.5$ MHz; the FWHM bandwidth of this event is $\delta f/f \approx 0.11$ and peak power is 3 10^{-18} W/m^2Hz. These correspond to peak values of about 10^{-16} V^2/m^2Hz for the MF emission and 3 10^{-17} V^2/m^2Hz for the HF. The background of the RAD2 instrument is given primarily by the spectrum of the galactic nonthermal continuum radiation at these frequencies. The emissions in Figure 2 are clearly not harmonic AKR [e.g. *Benson*, 1982], although there is harmonic substructure, spaced at $\delta f \approx 300$ kHz, visible in the AKR spectrum of the lower panel of Figure 2.

Assuming a source size, we can estimate the brightness temperature of the sources to compare with plasma thermal temperatures. At $6R_e$, the earth subtends a half-angle $\alpha \approx 9.5°$; assuming an unresolved source, the brightness temperature is given by $k_bT = \frac{c^2}{2f^2}\frac{F(f)}{\Delta\Omega}$, where F(f) is the measured flux density (from Figure 2) and $\Delta\Omega$ is the source size. Assuming emission from the disk of the earth, the MF emission has brightness temperature $T_{MF} \approx 2\ 10^{11}$ K, while the HF source gives $T_{HF} \approx 6\ 10^9$ K. If we take the source size to be 10 km in diameter (motivated below), the brightness temperatures are larger by a factor of 10^6. As there are no 10^9 K thermal plasmas in the magnetosphere, the emission must be nonthermal with an energetic particle population as the source.

On the other hand, if one assumes isotropic emission into a sphere, the ratio of peak power (of the MF component) to the background ($P_b \approx 1.5\ 10^{-18}$ W/m^2Hz) implies that the MF emission would be visible above background out to $\approx 22\ R_e$.

It is well known that the electron cyclotron maser instability (ECMI) generates intense z-mode emission at harmonics of the electron cyclotron frequency (f_{ce}) under certain conditions [e.g. *Winglee*, 1985; *Yoon et al.*, 1996; *Willes et al.*, 1998]. This process requires the presence of an unstable

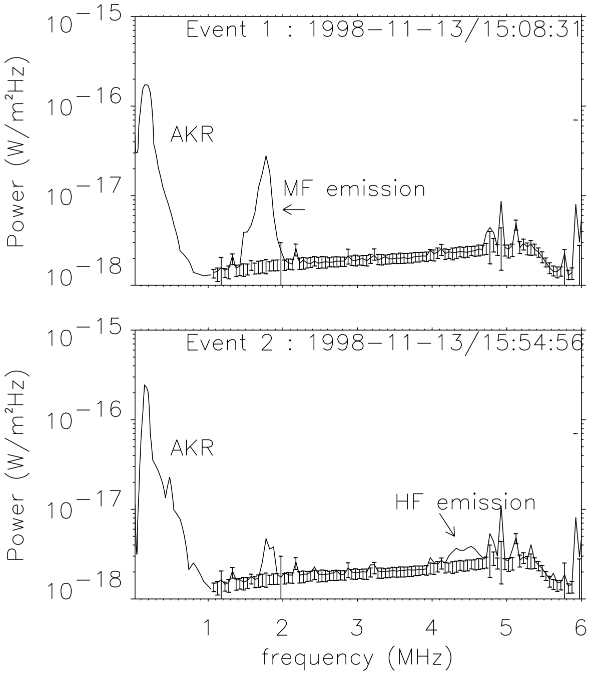

Figure 2. Power spectra during the MF (top) and HF (bottom) events from the RAD1 (0.02-1.04 MHz) and RAD2 (1.075-14 MHz) receivers. The MF emission in the top panel peaked at $f \approx 1.8$ MHz has bandwidth $\delta f/f \approx 0.14$ HF emission is peaked near $f_{HF} \approx 4.5$ MHz and has a similar FWHM bandwidth. The MF emission is still present during the HF event, at reduced power. Error bars on the RAD2 data are three standard deviations of the background.

perpendicular feature in the electron velocity distribution function ($\partial f/\partial v_\perp > 0$); a loss cone distribution is typically assumed. This interaction has been observed directly in the ionosphere [e. g. *Gough and Urban*, 1983]. The z-mode waves have a relatively small group speed and remained trapped in a layer near the generation region [*Willes et al.*, 1998]; the low group speed gives a large spatial growth rate as the waves remain near the source of free energy. However, to be observed at $6R_e$, or on the ground, these waves must couple to freely propagating x- or o-mode waves; this can be achieved by linear mode conversion in density structures or nonlinear mode conversion processes [*Weatherwax et al.*, 1995; *Willes et al.*, 1998]. The linear mode conversion mechanism was first discussed by *Ellis* [1956] and arises from scattering of the z-mode waves in density structures to tunnel to the o- and x-mode branches of the dispersion curve. The nonlinear mechanisms primarily involve the coalescence of z-mode waves to form freely propagating modes (e. g. $z + z \rightarrow x_2$) [*Willes et al.*, 1998]. In the case of auroral roar, recent observations have shown that the emission is polarized in the o-mode [*Shepard et al.*, 1997]; this observation seems to imply the linear mode conversion scenario as the z-mode couples preferentially into the o-mode in density gradients. Direct emission scenarios, have also been considered by several authors [*Weatherwax et al.*, 1995; *Yoon et al.*, 1996], but tend to produce x-mode radiation preferentially.

Figure 3 shows altitude profiles of the electron plasma frequency (f_{pe}), harmonics of the electron cyclotron frequency (f_{ce}, $2f_{ce}$, and $3f_{ce}$), and the upper hybrid frequency $f_{uh} = (f_{pe}^2 + f_{ce}^2)^{1/2}$. Electron density and magnetic field strength are taken from models (International Reference Ionosphere and International Reference Geomagnetic Field, respectively) at 75° invariant latitude, corresponding to the observed peak occurrence rate of auroral roar emissions [*Hughes and LaBelle*, 1998]. The electron density profile, and hence f_{pe} and f_{uh}, will vary considerably as a function of local time and magnetospheric and ionospheric conditions. In this way, Figure 3 is meant to be schematic rather than exact. Since the MF emission occurs at near 1.8 MHz, it is unlikely to have been generated on the bottomside ionosphere; the large density above would shield it from view by the spacecraft.

Assuming enhanced wave growth at cyclotron harmonics, and some electromagnetic coupling process linear or nonlinear, we propose that the 1.8 MHz MF emission is generated at $2f_{ce}$ where $f_{uh} \approx 2f_{ce}$ on the topside ionosphere. This occurs in two places (marked with solid circles in Figure 3) near 1000 km altitude, though the altitude will vary with ionospheric conditions. Likewise, the 4.4 MHz emission could be generated at $3f_{ce}$ where $f_{uh} \approx 3f_{ce}$; this condition is met near the density peak of the F layer at about 400 km and marked by a solid circle in Figure 3. Corresponding bottomside auroral roar emission regions are marked by open circles in the figure.

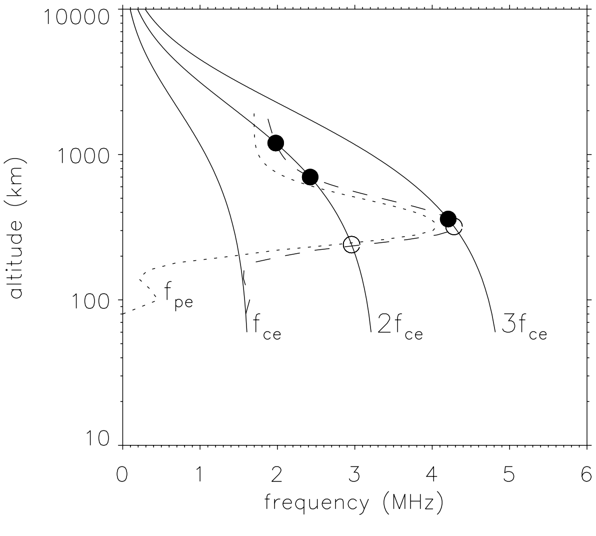

Figure 3. Characteristic frequencies vs. altitude from ionospheric density and field models. Solid lines are the electron cyclotron harmonics f_{ce}, $2f_{ce}$, and $3f_{ce}$. The plasma frequency (f_{pe}) and upper hybrid (f_{uh}) are dotted and dashed respectively. Since electrostatic wave growth is strongly enhanced where $f_{uh} = nf_{ce}$, we suggest that the observed waves are generated at n = 2 (MF) and n = 3 (HF) on the topside ionosphere. These correspond to altitudes of 1000 km and 400 km respectively. Solid circles show possible topside emission regions, while open circles show bottomside sources.

If the observed frequencies are cyclotron harmonics, we can infer the maximum extent of the source size parallel to the magnetic field from the bandwidth of the emission. For a dipole field $|\Delta f_{ce}/f_{ce}| = 3|\Delta r/r|$; using the bandwidths and altitudes from above, we find $\Delta r_{MF} \approx 47$ km and $\Delta r_{HF} \approx 15$ km, to be compared with the free space wavelengths of $\lambda_{MF} = 167$ m and $\lambda_{HF} = 68$ m respectively.

Summary

We report observations of MF and HF radio emission at 4-7 R_e by the WAVES experiment on the Wind spacecraft. The emission frequencies, $f_{MF} \approx 1.8$ MHz and $f_{HF} \approx 4.4$ MHz, imply an ionospheric origin and we suggest that the waves are generated on the topside ionosphere. The similarity in bandwidth, frequency, and structure suggests an analogy with bottomside auroral roar emissions. We propose that the emissions are generated by mode conversion (to o-mode) from z-mode waves generated by an electron cyclotron maser instability operating on a unspecified locally unstable electron distribution. We cannot, however, determine the polarization from our present observations.

The z-mode has the largest growth rate where the upper hybrid frequency matches harmonics of the electron cyclotron frequency ($f_{uh} \approx nf_{ce}$). Using ionospheric density and field models, we show that this occurs near 1000 km (MF) and 400 km (HF) under nominal conditions near 75° invariant latitude.

The MF emission begins first, with HF emission beginning roughly an hour later. It could be that we are seeing different emitting regions, with different characteristic frequencies. On the other hand, the F-layer density may be increasing with time, so emission switches from n=2 to n=3 as the F-layer peak approaches $3f_{ce}$ and $2f_{ce}$ becomes less than f_{uh}.

This observation seems to be quite rare; of 30 perigee passes by Wind, this is the first example of the phenomenon. Indeed, it seems to be the first convincing observation of radio emission from near the ionospheric F-layer beyond 0.5 R_e from earth. The emission may be beamed upward along auroral field lines, however, and the low inclination of the Wind spacecraft (prior to November 17, 1998) may have shielded it from more frequent observations. Ground-based auroral roar observations are much more common, though they are found to depend highly on local time and magnetic activity [*Hughes and LaBelle*, 1998]. Our observations occur during an interval of enhanced magnetic and ionospheric activity, which also explains the observed AKR.

Acknowledgments. Discussions with A. J. Willes, J. LaBelle, and P. J. Kellogg are acknowledged. Reference ionosphere (IRI) and magnetosphere (IGRF) models were obtained from the NSSDC at Goddard Space Flight Center. This work was supported by NASA grant NAG5-2815 to the University of California.

References

Benson, R. F., Harmonic auroral kilometric radiation of natural orgin, *Geophys. Res. Lett., 9*, 1120, 1982.

Bougeret, J.-L., et al., WAVES: The radio and plasma wave investigation on the Wind spacecraft, *Space Sci. Rev.*, *71*, 231, 1995.

Ellis, G. R., The Z propagation hole in the ionosphere, *J. Atmos. Terr. Phys., 8*, 43, 1956.

Gough, M. P., and A. Urban, Auroral beam/plasma interaction observed directly, *Planet. Space Sci.*, *31*, 875, 1983.

Hughes, J. M., and J. LaBelle, The latitude dependence of auroral roar, *J. Geophys. Res., 103*, 14,911, 1998.

James, H. G., E. L. Hagg, and D. L. P. Strange, Narrowband radio noise in the topside ionosphere, *AGARD Conference Proc.*, *138*, 24, 1973.

Kellogg, P. J., and S. J. Monson, Radio emissions from the aurora, *Geophys. Res. Lett., 6*, 297, 1979.

LaBelle, J., R. A. Treumann, M. H. Boehm, and K. Gewecke, Natural and man-made emission at 1.0-5.6 MHz measured between 10 and 18 R_e, *Radio Sci., 24*, 725, 1989.

Shepard, S. G., J. LaBelle, and M. L. Trimpi, The polarization of auroral radio emissions, *Geophys. Res. Lett., 24*, 3161, 1997.

Weatherwax, A. T., J. LaBelle, M. L. Trimpi and R. Brittain, Ground-based observations of radio emissions near $2f_{ce}$ and $3f_{ce}$ in the auroral zone, *Geophys. Res. Lett., 20*, 1447-1450, 1993.

Weatherwax, A. T., J. LaBelle, M. L. Trimpi, R. A. Treumann, J. Minow and C. Deehr, Statistical and case studies of radio emissions observed near $2f_{ce}$ and $3f_{ce}$ in the auroral zone, *J. Geophys. Res., 100*, 7745-7757, 1995.

Willes, A. J., S. D. Bale, and Z. Kuncic, A z-mode electron-cyclotron maser model for bottomside ionospheric harmonic radio emissions, *J. Geophys. Res., 103*, 7017, 1998.

Winglee, R. M., Fundamental and harmonic electron cyclotron maser emission, *J. Geophys. Res., 90*, 9663, 1985.

Yoon, P. H., A. T. Weatherwax, T. J. Rosenberg, and J. LaBelle, Lower ionospheric cyclotron maser theory: A possible source of $2f_{ce}$ and $3f_{ce}$ auroral radio emissions, *J. Geophys. Res., 101*, 27015, 1996.

Stuart D. Bale, Space Sciences Laboratory, University of California, Berkeley CA 94720-7450 USA (e-mail: bale@ssl.berkeley.edu)

(Received December 21, 1998; accepted January 14, 1999.)